ENERGY DISSIPATION IN THE AXIAL FAN TIP CLEARANCE FLOW

Matej MILAVEC [1], Stane PIVK [1],
Daniel VIDAL de VENTÓS [1], Branko ŠIROK [2], Benjamin BIZJAN [3]

*[1] HIDRIA d.o.o., Fan & Blowers, Spodnja Kanomlja 23,
5281 Spodnja Idrija, Slovenia*

*[2] University of Ljubljana, Faculty of Mechanical Engineering (FME),
Aškerčeva 6, 1000 Ljubljana, Slovenia,*

[3] ABELIUM d.o.o., Kajuhova ulica 90, 1000 Ljubljana, Slovenia

SUMMARY

This paper presents a study of velocity and pressure fluctuations in the axial fan tip clearance flow for two different blade tip designs. A standard blade tip design was compared to the modified design in which the tip was curved in a fold-like shape. A comparison of integral sound parameters indicates a significant noise level reduction for the modified blade tip design. Also presented is a new experimental analysis method based on the simultaneous measurements of local velocity and pressure. The method allows the results to be presented in the phase space with the possibility of turbulent flow properties characterization and flow structure identification.

INTODUCTION

Air gap of an axial fan is the region in the flow path of the fan that connects the rotational domain of rotor and the stationary domain at which the ventilator is built up. Because of the fact that it prevents contact between blades and the stationary fan housing, it represents a connection between over- and under pressure regions of ventilator blade sides. Due to pressure differences around the blade tip there is a fluid flow that goes from over- to underpressure side of the blade, which joins the main axial stream flow that flows between blade spaces, in the form of fluid vortices at the peripheral region of the ventilator flow path. Vortex structures that are generated in the peripheral region of the ventilator's blade are called also induced vortices. The latter is one of the mechanisms of the rotating blade that creates induced resistance. In interaction with the stationary housing of the ventilator, this forms a leakage fluid flow, which is characterized by high velocity gradients and related energy dissipation effects. Air gap depth and the shape of its boundary layer significantly influence the integral aerodynamic and acoustic characteristic of the ventilator.

The air gap region and induced vortices are topics that have been studied by many authors. First studies were presented by Rains [1], Vavra [2] and Senno and Ishida [3], who described this flow leakage based on theoretical pressure distribution. Their models were later improved several times. The characterization of vortices in the blade tip region was performed by developing phenomenological models by Lakshminarayana and Horlock [4]. Formation of vortex/turbulence structures behind the blade tip were defined as potential vortices to describe induced resistance, which can be roughly used to describe losses in the mid region of the blades. The model was further improved and experimentally validated (Inoue [5]). Subsequently, studies were carried out in which it was determined that the leakage in the tip's blade area may be the dominant source of broadband noise (Longhouse [6]). By measuring the pressure and velocity fluctuations in the air gap region, Longhouse also discovered the presence of discrete frequencies lower than the frequency of the blade passage, which could consequently be related with the flow separation at the blade tip. For acquisition of the phenomenological data a microphone and an anemometer were used. In the recent studies, authors have focused on the use of numerical analysis of different blade tips that reduce the intensity of the flow and turbulence after the tip (Corsini in Sheard [7], Corsini [8], Bianchi [9]). Most of the studies were carried out in a wind tunnel on profiled blades that ended with the blade tip.

In the present article, a new method of treating the leakage flow and induced vortices is presented. Measured pressure and velocity fields in the region of the air gap have been phase-averaged and are presented in form of attractors, which describe the dependence of pressure and velocity fluctuations as potential sources of dissipation of mechanical energy and generation of turbulent noise of the ventilator.

EXPERIMENTAL WORK

To research the influence of the blade tip shape on the axial fan operation, we used a fan designed and manufactured by Hidria. Blade profile is designed according to NACA profile model in combination with parameters set up by the manufacturer Hidria. The blade construction is designed so that the upper blade part (tip) with diameter D_{LT} can be exchanged. The blade tip represents the only geometric change of the blade on the tested fan (Fig. 1). Two different blade tip shapes were used and will be denoted as shapes A and B. Technical and geometric properties of the fan common to all experiments are presented in Table 1.

Table 1: Technical properties of testing fan

$D_{exterior}$	0.635	[m]
$D_{interior}$	0.135	[m]
D_{LT}	0.6	[m]
d_0: air gap depth (Fig. 3, detail E_1)	0.004	[m]
N_b no. blades	5	
Tip's profile	NACA	
Electric motor	HEC-R10	
f_0: rotational frequency	650	[min^{-1}]

The winglet's shape (Fig. 1) of type A represents an extension of the basic blade geometry all the way to the tip of the blade. In the case of the winglet type B, the geometry of the blade tip is homogenously curved towards the under pressure side. The minimum average air gap d_0 between the blade tip and the housing is the same for both tested blade winglets.

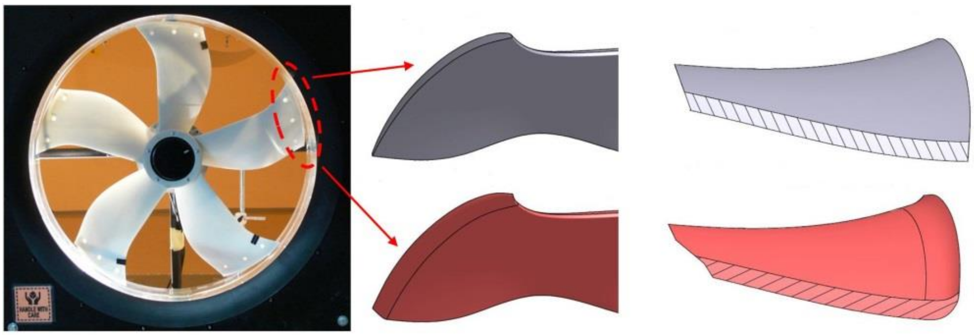

Figure 1: Test fan (left) in which the location of the change in geometry is marked. In the middle, two different shapes of blade winglet are shown from top to bottom (type A and type B, respectively). On the right, the shape of the blade cross-section is shown

INTEGRAL MEASUREMENTS OF AERODAYNAMIC AND ACOUSTIC CHARACTERISTICS

The measurement process of aerodynamic and acoustic characteristics of the ventilator are described in detail in the article [10]. The influence of the winglet on the integral characteristic $\psi(\varphi)$ can be detected mainly in the region of smaller pressure numbers ψ, with the increase in the number ψ decreasing the difference to within the range of the measurement uncertainty of the measuring system. The difference between results of the measured sound power L_{WA} is characteristic throughout the field of the acoustic characteristics of the fan. The largest measured sound power difference of 8.6 dB(A) was detected at the point of the fan's maximum aerodynamic efficiency.

In Fig. 2 the frequency spectrum of the sound pressure level L_p measured in a reverberant chamber [10] is presented for both shapes of blade tip. With the aid of the coefficient of the intensity decay α in the frequency spectrum, it is possible to identify and evaluate the noise generation mechanisms and the properties of the flow kinematics [11]. In addition to the measured frequency spectrum of the sound pressure after blade tip for tip shapes A and B, lines are also plotted in Fig. 2 which illustrate the dependence of the sound pressure amplitudes over the frequency. For the decay of the isotropic turbulence according to Zhou-Rubinstein, the slope decline is $\alpha = -4/3$, and for a signal of sound pressure level that is characterized by anisotropic turbulence decay [11] the corresponding slope decline is given by $\alpha = -10/3$. For comparison, in Fig. 2 a line with a decay slope of $\alpha = -2.8$ is also plotted. This line was determined experimentally for the case of sound pressure emission in a freely discharging jet of air from the nozzle, where the so-called shear turbulence was predominant. The slope decay $\alpha = -2.8$ was calculated by Rubinstein and Zhou [11], and Tama and Golebiowskega [12] from measurements. The authors Tam and Golebiowski tested different shapes of nozzles, where they considered the noise of the outlet air in cases of subsonic and supersonic speeds. They found that the compressibility of the medium (air), neither at subsonic nor at supersonic speeds does not significantly affect the turbulent generation of noise, except near the speed of sound. This finding was experimentally confirmed by Papamoschou and Roshko [13] and Bogdanoff [14]. The experimentally determined decay coefficient of the sound pressure signal measured by Tam et al. [13] coincides in its form with the measured frequency spectrum for a frequency range above 2200 Hz and for the shape of the blade tip A. The slope of the line, which is measured for the shape of the blade tip A, is also very similar to the value of the coefficient of the theoretically determined line, which determines the decay in the sound pressure signal with frequency to indicate the presence of anisotropic turbulence.

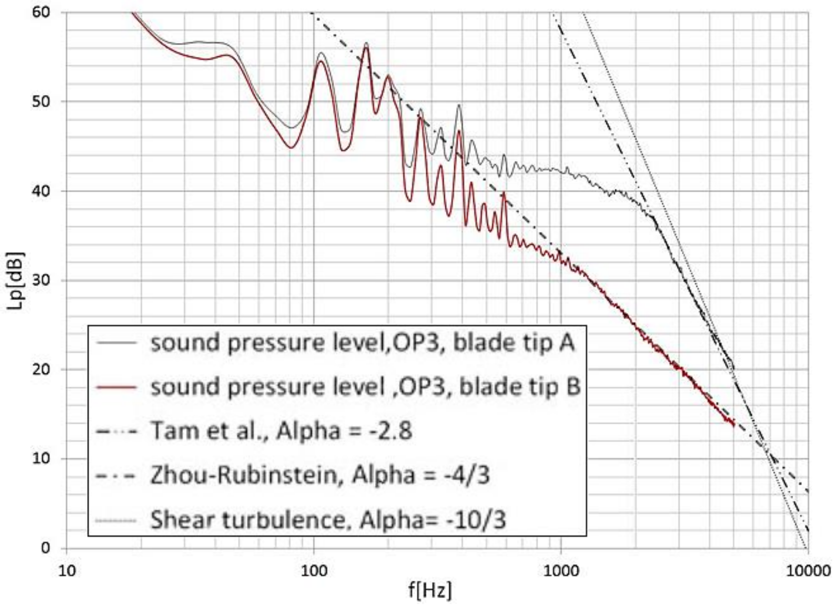

Figure 1: Frequency spectrum of sound pressure in the range from 11.7 Hz to 5000 Hz for fan with shapes of blade tip A and B in operating points OP-A in OP-B. OP3 belongs to maximal working point of fan efficiency.

In order to understand the measurement results at an integral level and to describe flow phenomena around the blades, local measurements of the sound pressure and velocity were carried out in the region of the air gap. Measurements were performed in the maximum efficiency operating points of the ventilator for both shapes of the blade tip (A and B).

To facilitate the measurements, the test fan (Fig. 3, item 7) was installed in a fan housing (item 6), which consisted of a metal plate (item 5) that was used to attach the housing to the rectifier wall [10]. The input radius of the housing (Fig. 3, Item 6) was manufactured using selective laser sintering technology (SLS) and was the connecting element between the transparent housing and the metal plate. In the housing, measurement points (outlets) were designed to monitor the pressure fluctuations (Fig. 3, detail C) and velocity fluctuations (Fig. 3, detail E). These two measurements points enabled the installation of aligned sensors i.e. without changing the thickness and additional changes in the geometry of the air gap. The provided air gap thickness (d_0 = 4 mm) represents the average shortest distance between tip of the blade and housing of the ventilator (shroud).

Measurements of pressure fluctuations *p* in the air gap were performed with the surface microphone G.R.A.S. 40PS (Fig. 3, detail C). The microphone was powered by an external power supply G.R.A.S. Type12AL (Fig. 3, item 2) and connected to the DA data acquisition system (Fig. 3, item 4). We used a 16-bit measurement card to capture the data with a sample frequency of 50 kHz. The entire measuring chain was connected to a computer (Fig. 3, item 3). The total data capture time was limited to 10 s. Measurements of velocity fluctuations in the air gap region were made with a one-dimensional hotwire anemometer system Dantec mini CTA, using a sensor type 55P11 (Fig. 3, detail E). We used a low-pass filter with a cutoff frequency of 10 kHz (Fig. 3, item 1). Measurements of velocity and pressure fluctuations were performed simultaneously with a sampling frequency of 50 kHz by recording time lengths of $4.25 \cdot 10^5$ points. The measuring sensor was set at a distance of 1 mm from the inner face of the transparent ring-shaped fan housing (Fig. 3, item 8), which corresponded to 1/4 of the total air gap d_0.

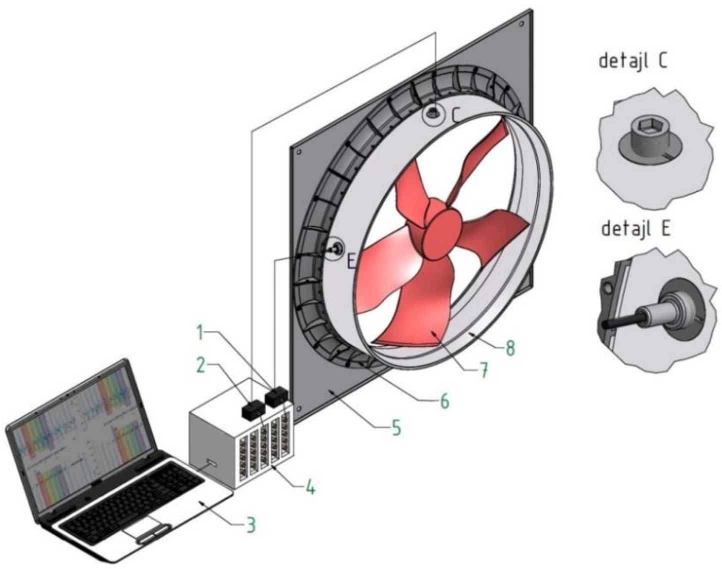

Figure 2: Local pressure and velocity measurement set-up

ANALYSIS

Differences in the frequency spectrum of the sound pressure for the winglets A and B in Fig. 2 are the consequence of leakage flow in the air gap between blade and housing. Fluctuations of velocity ($v(t)$) and pressure ($p(t)$) affect the emitted sound pressure. Parametric representation of these two variables $\{v(t), p(t)\}$ shows a mutual phenomenological dependence of velocity and pressure conditions. With the occupancy of the pair $\{v(t), p(t)\}$ in the phase space, a structure of the attractor is defined, characterizing the occurrence of turbulent kinetic energy dissipation depending on the position of the blade relative to the selected measurement point on the housing. The occupancy density of the phase space will be denoted by $n(v, p)$, where n is the number of samples (events) in the selected phase space over the entire duration of the measurement. The phase space is divided into segments with 1.9 Pa step at the pressure axis and 0.09 m/s step at the velocity axis. In Figs. 4 A and B, the occupancy density of the phase space $n(v, p)$ is shown by a color surface plot.

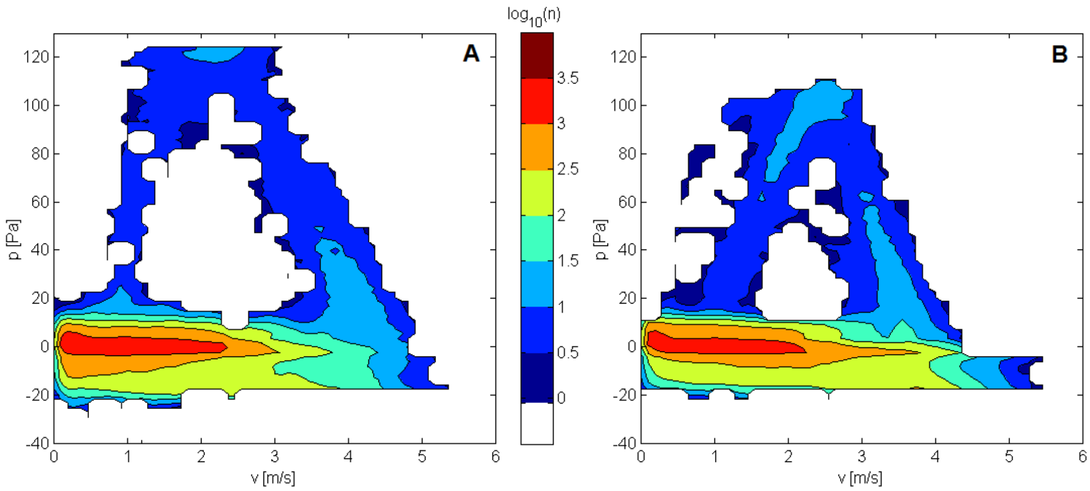

Figure 4: n(v, p), for fan's winglet shapes A (left) in B (right)

Using the density of occupancy of the phase space n, the energy level E can be determined as the product $E(v, p) = v \cdot p \cdot n(v, p)$, which is proportional to the emitted energy per unit area in the leakage flow. As such, it enables identification of significant sources of dissipation of turbulent kinetic energy, which appears as a characteristic source of the fan's acoustic emission. In Figs. 5 A and B, the energy level $E\ (v, p)$ is represented by a color surface plot, and the thick black line denotes the time average attractor *(v, p)*. Thus, from the diagrams *n(v, p)* and *E(v, p)* we can make conclusions about the intensity of dissipation of turbulent kinetic energy. In both cases (geometry A and B) we observe a similar structure of the distribution of the variable *E(v, p)*. In the upper part of the diagram, there is a periodic structure resulting from the passage of the blade surface through the pressure and velocity sensors.

Amplitudes of corresponding velocity and pressure fluctuations are lower in the case of the winglet B (Fig. 4 B and Fig. 5 B) than for the winglet A (Fig. 4 A and Fig. 5 A). The phase space occupancy is lower with less pronounced mechanical energy, which coincides with the smaller emitted sound pressure in the frequency range from 100 to 200 Hz in the diagram in Fig. 2.

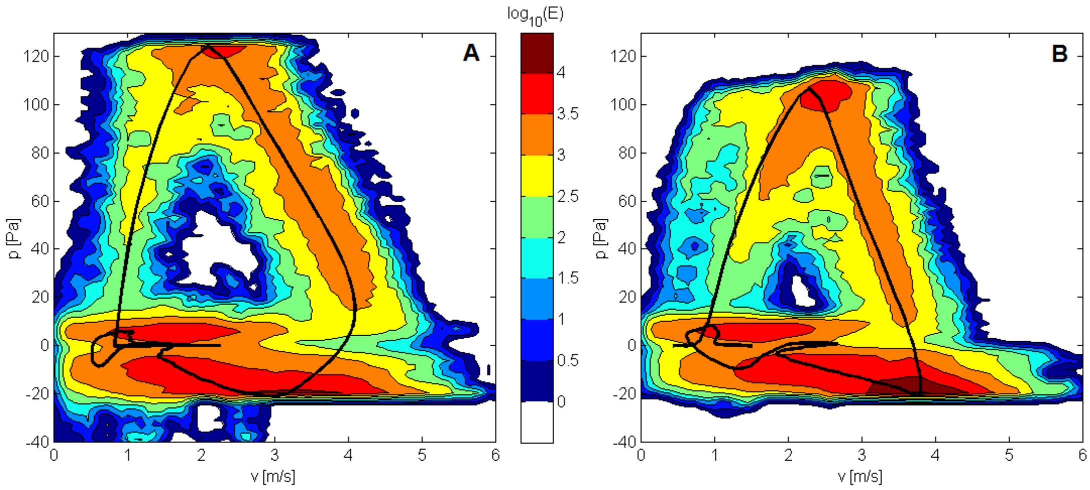

Figure 5: E(v, p), for fan's winglet shapes A (left) in B (right)

The lower part of the diagrams of Figs. 4 and Fig. 5 is located in the area of large velocity (0 to 6 m/s) and small pressure fluctuations (from -20 to 20 Pa). This area belongs to the dissipation of turbulent kinetic energy, which is characterized by generating aerodynamic losses and high-speed turbulent noise. In this area, large coherent vortex structures that are a consequence of the leakage flow between the blade and the housing break down into smaller vortices, as shown in Fig. 2 and represented by the frequency spectrum in the range of 1 kHz to 5 kHz. When comparing the diagrams in Fig. 4 and Fig. 5, it can be concluded that the emitted mechanical energy is greater in the case of the winglet A in Fig. 4 and Fig. 5. This implies a smaller presence of larger vortex structures in the upper part of diagrams in Fig. 4 and Fig. 5, and consequently also less accentuated fluctuations in the lower part of diagrams in Fig. 4 and Fig. 5. The dissipation of mechanical energy for both widget shapes can also be compared quantitatively by integrating time-averaged values *(v, p)* per fan rotation at a frequency f_0. We obtain the intensity of the scattered energy flow *j* (eq. 1):

$$j = f_0^{-1} \cdot \oint p \cdot dv. \qquad (1)$$

For blade tip A we obtain j = 280 W/m^2, and for blade tip B j = 191 W/m^2, meaning a decrease of 32 % of local emitted energy flux or 1.7 dB when geometry is changed from shape A to B.

From presented results we can conclude that the shape of the blade is important for both the formation of large vortex structures beyond winglet as well as for the stability of flow conditions and less accentuated dissipation of the kinetic energy in the flow after the blade winglet. Both phenomena have a significant effect on the generation of turbulent noise on axial fans, which is confirmed by shown trends of the spectrum of the sound pressure in Fig. 2. The corresponding decrease of the emitted sound pressure level depends on the shape of the winglet and the size of the air gap between the blade and the ventilator housing.

CONCLUSIONS

The article investigates the effect of the blade tip shape of an axial fan on noise emission due to turbulent energy dissipation and local airflow kinematics, for two distinctly different blade tip (winglet) geometries. The winglet shape A represents the basic extension of the blade profile geometry, which ends in the region of the air gap. The winglet shape B defines a softer passage of the blade surface from the over-pressure side to the under-pressure side, with both sides joining in the form of a wedge on the suction (under-pressure) side of the blade.

The measured frequency spectrum of the sound pressure signal is significantly lower in the case of the blade tip shape B in the higher frequency range, which is also reflected in a lower integral sound pressure level of the fan. The difference in the course of sound pressure spectra was analyzed based on results of simultaneous measurements of velocity and pressure fluctuations, whereby the dissipation of turbulent kinetic energy was estimated in local regions of the phase space and on an integral level.

Regions of coherent vortices and decay were identified in the leakage flow between the winglets and the fan housing. In the case of blade tip shape B, where the tip geometry was uniformly wound in the direction of the pressure side of the blade, formation of coherent vortices structures as well as dissipation of turbulent kinetic energy is less pronounced, which is also reflected on the integral level by reduced emitted sound power.

REFERENCES

[1] D. A. Rains – *Tip clearance flows in axial flow compressors and pumps*. California institute of technology, Hydrodynamics and mechanical engineering laboratories, Report No. 5, California, **1954**

[2] M. H. Varva – *Aerothermodynamics and flow in Turbomachines*. John Wiley & Sons, New York, **1960**

[3] Y. Senoo, M. Ishida – *Pressure loss due to the tip clearance of impeller blades in centrifugal and axial blowers*. J. Eng. for gas turbines and power, 108, p. 32-37, **1986**

[4] B. Lakshminarayana, J. H. Horlock – *Tip-clearance flow and losses for an isolated compressor blade,* British ARC R & M 3316, **1962**

[5] M. Inoue, M. Kuroumaru, M. Fukuhara – *Behavior of tip leakage flow behind an axial compressor rotor*. J. Eng. Power, 108(1), p. 7-14, **1986**

[6] R. E. Longhouse – *Control of tip-vortex noise of axial flow fans by rotating shrouds*. Journal of sound and vibration, 58, p. 201-214, **1978**

[7] A. Corsini, A. G. Sheard – *Tip end-plate concept based on leakage vortex rotation number control.* Journal of computational and applied mechanics, 8, p. 21-37, **2007**

[8] A. Corsini, F. Rispoli, A. G. Sheard - *Development of improved blade tip end plate concepts for low-noise operation in industrial fans*. Journal of power and energy, 221, p. 669-81, **2007**

[9] S. Biannchi, A. Corsini, F. Rispoli, A. G. Sheard – *Experimental development of a measurement technique to resolve the radial distribution of a fan aero-acoustic emissions*. Noise control engineering journal, 57, p. 360-369, **2009**

[10] M. Milavec, B. Širok, M. Hočevar, S. Pivk, E. Pavlovič – *Influence of the shape of the blade tip on the emitted noise in the air-gap between the rotor and the housing of an axial fan*. Forschung im Ingenieurwesen, **2014**

[11] R. Rubinstein, Y. Zhou - *Time correlations and the frequency spectrum of sound radiated by turbulent flows*. Institute for Computer Applications in Science and Engineering NASA Langley Research Centre, **1997**

[12] C. K. W. Tam, M. Golebiowski - *On the two components of turbulent mixing noise from supersonic jets.* NASA Langley Research Centre, **1996**

[13] D. Papamoschou, A. Roshko - *The compressible turbulent shear layers: An experimental study, Fluid Mechanics, 197, p. 453-477*, **1988**

[14] D. W. Bogdanof - *Compressible effects in turbulent shear layers. AIAA J., 21, p. 26-927*, **1988**